

Control of extraordinary light transmission through perforated metal films using liquid crystals

Y.M. Strelniker^{1,a}, D. Stroud², and A.O. Voznesenskaya³

¹ Minerva Center, Jack and Pearl Resnick Institute of Advanced Technology, and Department of Physics, Bar-Ilan University, 52900 Ramat-Gan, Israel

² Department of Physics, The Ohio State University, Columbus, Ohio 43210, USA

³ St. Petersburg State University of Information Technologies, Mechanics and Optics, St. Petersburg 197101, Russian Federation

Received 27 December 2005 / Received in final form 18 May 2006

Published online 6 July 2006 – © EDP Sciences, Società Italiana di Fisica, Springer-Verlag 2006

Abstract. We calculate the effective dielectric tensor of a metal film penetrated by cylindrical holes filled with a nematic liquid crystal (NLC). We assume that the director of the NLC is parallel to the film, and that its direction within the plane can be controlled by a static magnetic field, via the Freedericksz effect. To calculate the effective dielectric tensor, we consider both randomly distributed holes (using a Maxwell-Garnett approximation) and a square lattice of holes (using a Fourier technique). Both the holes and the lattice constant of the square lattice are assumed small compared to the wavelength. The films are found to exhibit extraordinary light transmission at special frequencies related to the surface plasmon resonances of the composite film. Furthermore, the frequencies of peak transmission are found to be substantially split when the dielectric in the holes is anisotropic. For typical NLC parameters, the splitting is of order 5–10% of the metal plasma frequency. Thus, the extraordinary transmission can be controlled by a static magnetic or electric field whose direction can be rotated to orient the director of the NLC. Finally, as a practical means of producing the NLC-filled holes, we consider the case where the entire perforated metal film is dipped into a pool of NLC, so that all the holes are filled with the NLC, and there are also homogeneous slabs of NLC on both sides of the film. The transmission in this geometry is shown to have similar characteristics to that in which the NLC-filled screen is placed in air.

PACS. 78.67.-n Optical properties of low-dimensional, mesoscopic, and nanoscale materials and structures – 78.66.Sq Composite materials

1 Introduction

The recent discovery [1,2] of “extraordinary transmission” of light through a metal film perforated by a periodic array of sub-wavelength holes has stimulated worldwide interest. This transmission is widely believed to result from the coupling of light to plasmons on the surface of the patterned metal film [2–4]. At particular wavelengths, this coupling is exceptionally strong, permitting a very high fraction of incident light energy to be transmitted through the film. This proportion can far exceed the areal fraction of holes on the metal film surface.

In a recent paper [5], it was shown that a magnetic field applied parallel to the film would significantly alter this transmission. The alteration occurs because the magnetic field makes the metal dielectric tensor anisotropic. The effective dielectric tensor $\epsilon_e(\omega)$ of the composite film also becomes anisotropic, and the frequencies of the surface plasmons (SP’s) are shifted, as is the frequency of

the peak transmission. These calculations are carried out in the long wavelength limit, in which the distance between the holes is small compared to a wavelength. Under these circumstances, the optical properties of the film can be treated in terms of an effective film dielectric tensor. Unfortunately the materials like Ag, Au, Al, traditionally used in extraordinary light transmission studies, can not be used for such magnetic field sensitive devices, since in such materials the dimensionless magnetic field $H \equiv \omega_c \tau = \mu B$ is very small due to low electronic mobility μ (here $\omega_c = eB/me$ is the cyclotron frequency, τ is the conductivity relaxation time, B is the magnetic field measured in conventional unites [6–8]). In order to see the effect of a static magnetic field on the value of the plasmon frequency ω_p , in reference [5] it was proposed to use semiconductor materials like GaAs and InAs. The idea to use the magnetic field in order to affect the surface plasmons and therefore to control the light propagation is used also in references [9–16].

In this paper, we extend this idea to perforated metal film (made from metals traditionally used in such cases,

^a e-mail: strelnik@mail.biu.ac.il

such as Ag, Au, or Al), whose holes are filled by a uniaxially anisotropic dielectric, such as a nematic liquid crystal (NLC). NLCs strongly affect the optical properties of various inhomogeneous dielectrics. For example, the photonic band gap of a periodic dielectric infused with the NLC can be tuned, and even made to close, by suitably orienting the principal axis \hat{n} of the NLC, known as the director, with an electric field [17]. Similarly, the SP frequencies of both random distributions and chains of small metal particles are altered when these systems are immersed in the NLC [18–22]. For the present application, we assume that \hat{n} is perpendicular to the hole axis [23]. For this film, we again find that the transmission peak is shifted by the anisotropy, and is split for different polarizations of incident light. Since \hat{n} can be rotated by changing the direction of an applied static magnetic field \mathbf{H}_0 (see Fig. 1a) (so-called magnetic Fredericksz effect [25,24]), this result implies that the transmission can be controlled simply by rotating \mathbf{H}_0 even if this magnetic field has no effect on plasma frequency ω_p of the metallic film (like Ag, Au, Al, etc.).

Another, technically more convenient method to control light transition, is using of an electric field \mathbf{E}_0 . For this, we can take the entire metal-perforated film and dip it into a large pool of the NLC (see Fig. 1b). Thus, all the holes are filled with NLC, and there are also layers of NLC on both sides of the film. Then it is easy to align the NLC director within the holes by applying a static electric field \mathbf{E}_0 (so-called electric Fredericksz effect [25,24]) along the film plane, e.g., in x -direction. This will align the NLC in the holes, and also in the medium on either side of the film (see Fig. 1b). Then it is easy to re-align the NLC director in another direction, e.g., along z -axis just by applying a static electric field \mathbf{E}_0 in this direction. It is still possible to calculate the transmission as a function of the orientation of the electric field relative to the hole lattice. The only difference in the calculation is that one has three anisotropic layers instead of just one in the previous case. This geometry shows that the system we envision can be prepared physically.

The remainder of this paper is arranged as follows. In Section 2, we describe our method of calculating the effective permittivity tensor $\hat{\epsilon}_e$ for both random and ordered arrangements of cylindrical holes in a metallic film. In Section 3, we present numerical results for both cases, based on these expressions, followed by a brief discussion in Section 4.

2 Formalism

Let us consider a geometry which corresponds to the above-mentioned experiment [1–3]: a metal film, with a square array of identical perpendicular cylindrical holes, is placed in a static, in-plane magnetic \mathbf{H}_0 (or electric \mathbf{E}_0 field) whose direction can be rotated within the xz plane (see Fig. 1). A monochromatic light beam, of angular frequency ω , impinges upon this film along the perpendicular axis y , with linear polarization along the principal axis x of the array — see Figure 1.

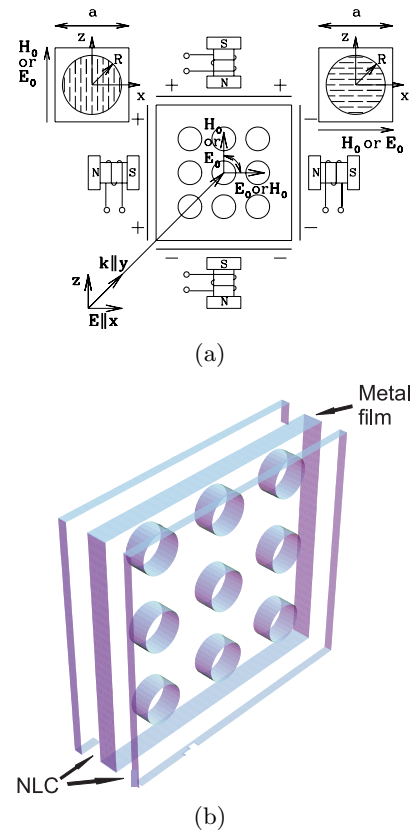


Fig. 1. (a) Schematic drawing of a metal film with a periodic array of holes filled with a NLC whose director is parallel to the film and can be rotated in the film plane by a static magnetic, \mathbf{H}_0 , (or electric \mathbf{E}_0) field. The coordinate axes x , y , z , are always directed along the principal axes of the simple square lattice, and the applied static magnetic field \mathbf{H}_0 (created by a system of solenoids) always lies in the film plane. The incident light beam is normal to the film surface, i.e., the ac electric field \mathbf{E} is parallel to the film plane, while the wave vector is normal to it (i.e., $\mathbf{k} \parallel y$). Note that the ac magnetic field \mathbf{B} of the light wave ($\mathbf{B} \perp \mathbf{E}$) is not important in our considerations and we omit it everywhere. Insets: the $a \times a$ unit cell of the periodic composite film with a cylindrical hole of radius R filled with a NLC whose director is parallel to the film and can be rotated by application of a static magnetic \mathbf{H}_0 (or electric \mathbf{E}_0) field whose direction can be rotated within the xz -plane. (b) (Color online) Schematic drawing of a metal film perforated by a square array of holes and dipped into a pool of NLC. The center layer (shaded, with circular holes) represents the metal film; the other two layers represent homogeneous layers of NLC.

We first consider a single cylindrical hole in a metallic host (see inset to Fig. 1). The hole is assumed parallel to the y axis, and filled with an anisotropic material having a dielectric tensor with principal components ϵ_{ii} , ($i = x, y, \text{ or } z$). In the calculations shown below, we consider $\epsilon_{zz} \neq \epsilon_{xx} = \epsilon_{yy}$. The host has an isotropic complex, and frequency-dependent dielectric constant $\epsilon_m(\omega)$. To compute the frequency of an SP bound to the hole, we consider an applied uniform ac electric field \mathbf{E} (i.e., the

electric field of the incident electromagnetic wave). Then the electric field \mathbf{E}_{in} within the hole is also uniform and may be written [5, 8, 26–30]

$$\mathbf{E}_{in} = \hat{\gamma} \cdot \mathbf{E}, \quad (1)$$

where $\hat{\gamma}$ is a 3×3 matrix, diagonal in the (x, y, z) coordinate system, with components $\gamma_{yy} = 1$,

$$\gamma_{xx} = \frac{\epsilon_{xx}}{\epsilon_{xx} - n_x \delta \epsilon_{xx}}, \quad \gamma_{zz} = \frac{\epsilon_{zz}}{\epsilon_{zz} - n_z \delta \epsilon_{zz}}. \quad (2)$$

Here, $\delta \epsilon_{ii} = \epsilon_m - \epsilon_{ii}$, and the quantities n_x and n_y are depolarization factors given by

$$n_y = 0, \quad n_x = \frac{1}{1 + \sqrt{\epsilon_{zz}/\epsilon_{xx}}}, \quad n_z = 1 - n_x. \quad (3)$$

For simplicity, we assume the host has a Drude dielectric function,

$$\epsilon_m = 1 - \frac{\omega_p^2}{\omega(\omega + i/\tau)}, \quad (4)$$

where $\omega_p = (4\pi n_0 e^2/m)^{1/2}$ is the plasma frequency (n_0 is the density of charge carriers, e is the charge of one carrier, and m is its effective mass, see references [8, 26]) and τ is a relaxation time. We consider the limit $\omega_p \tau \rightarrow \infty$. The frequency $\omega_{sp,i}$ of the SP polarized in the i th direction is that frequency where \mathbf{E}_{in} (see Eq. (1)) becomes very large even for a very small applied field. This condition is satisfied when

$$\epsilon_{m,ii}(\omega_{sp,i}) - n_i \delta \epsilon_{ii}(\omega_{sp,i}) = 0. \quad (5)$$

For example, $\omega_{sp,x}$ satisfies the equation

$$\epsilon_m - \frac{\epsilon_{xx} - \epsilon_m}{1 + \sqrt{\epsilon_{m,zz}/\epsilon_{m,xx}}} = 0. \quad (6)$$

Substituting equation (4) into this and similar written for y -direction expressions, and letting $\omega_p \tau \rightarrow \infty$, one obtains

$$\omega_{sp,x} = \frac{\omega_p}{\sqrt{1 + \epsilon_{xx}}}, \quad \omega_{sp,z} = \frac{\omega_p}{\sqrt{1 + \epsilon_{zz}}}. \quad (7)$$

As an example, suppose that the material within the hole is the NLC known as BEHA (p-butoxyphenyl ester-p'-hexyloxybenzoic acid [31]), an uniaxial dielectric with principal dielectric constants 1.96, 1.96, and 2.56 [32]. If $\hat{n} \parallel \hat{x}$, then equations (3) show that the SP frequencies are split in this case by $\sim 0.06\omega_p$. The dimensions of the NLC molecules are typically ~ 20 Å in length and ~ 5 Å in width [24, 31], which are small compared to the typical dimensions of the holes used in experiments ($d \sim 150$ – 400 nm) as well as typical film thickness ($h \sim 300$ nm, see Refs. [1–4, 33]) used in extraordinary light transmission experiments. (The dimensions of the holes should also be small compared to the wavelength of light, in order for the theory given below to be rigorously applicable. Possible effects arising from larger hole dimensions are briefly discussed below).

Next, we approximately compute the tensor $\hat{\epsilon}_e(\omega)$. The film is appropriately described by $\hat{\epsilon}_e$ if it is homogeneous on a scale of the electromagnetic wavelength. If the holes form a periodic lattice, as in experiments, this description is suitable provided the lattice constant is much less than a wavelength. The effective permittivity tensor $\hat{\epsilon}_e(\omega)$ is defined by the relation

$$\hat{\epsilon}_e \langle \mathbf{E}(\mathbf{x}) \rangle = \langle \hat{\epsilon}(\mathbf{x}) \cdot \mathbf{E}(\mathbf{x}) \rangle, \quad (8)$$

where $\langle \dots \rangle$ denotes a volume average, and $\hat{\epsilon}(\mathbf{x})$ is the local dielectric tensor. We now discuss the calculation of $\epsilon_e(\omega)$ in several regimes.

First, we consider a dilute collection of parallel, right-circular cylindrical inclusions. For a dilute suspension of inclusions, the tensor $\hat{\epsilon}_e$ takes the form [30]

$$\hat{\epsilon}_e = \hat{\epsilon}_m - p \delta \hat{\epsilon} \cdot \hat{\gamma}, \quad (9)$$

where p is the volume fraction of inclusions. For the present geometry under consideration, where the symmetry axes of the cylinder and the NLC are perpendicular, $\hat{\epsilon}_e$ takes the form

$$\epsilon_{e,ii} = \epsilon_m \left[1 - p \frac{\delta \epsilon_{ii}}{\epsilon_m - n_i \delta \epsilon_{ii}} \right], \quad (10)$$

where $i = x, y, z$, n_x and n_z are given by equations (3) and $n_y = 0$.

In Maxwell-Garnett (MG) (or Clausius-Mossotti) approximation [27, 28], equation (10) takes a slightly different form:

$$\epsilon_{e,ii} = \epsilon_m \left[1 - p \frac{\delta \epsilon_{ii}}{\epsilon_m - n_i(1-p)\delta \epsilon_{ii}} \right]. \quad (11)$$

The analog of equation (5) is $\epsilon_m - n_i(1-p)\delta \epsilon_{ii} = 0$, from which in the limit $\omega_p \tau \rightarrow \infty$ we obtain the following expression for ω_{sp} :

$$\omega_{sp,x} = \frac{\omega_p}{\sqrt{\left[\frac{1}{n_x(1-p)} - 1 \right] + \epsilon_{xx}}}, \quad (12)$$

$$\omega_{sp,z} = \frac{\omega_p}{\sqrt{\left[\frac{1}{n_z(1-p)} - 1 \right] + \epsilon_{zz}}}. \quad (13)$$

The resonant frequency now depends on the volume fraction of the holes, p . In the dilute limit ($p \rightarrow 0$), expressions (12), (13) reduce to equations (7).

In a typical experiment (e.g. those reported in Refs. [1] and [2]), the cylindrical holes are arranged on a two-dimensional periodic (usually a square) lattice. In this case, the MG approximation is no longer the most accurate method for calculating the tensor $\hat{\epsilon}_e(\omega)$. A more suitable approach is to use a Fourier expansion technique, as done, e.g., in reference [5]. This approach is readily carried out numerically, and the resulting $\hat{\epsilon}_e$ can be computed for an arbitrary orientation of \hat{n} within the plane normal to the cylinder axes.

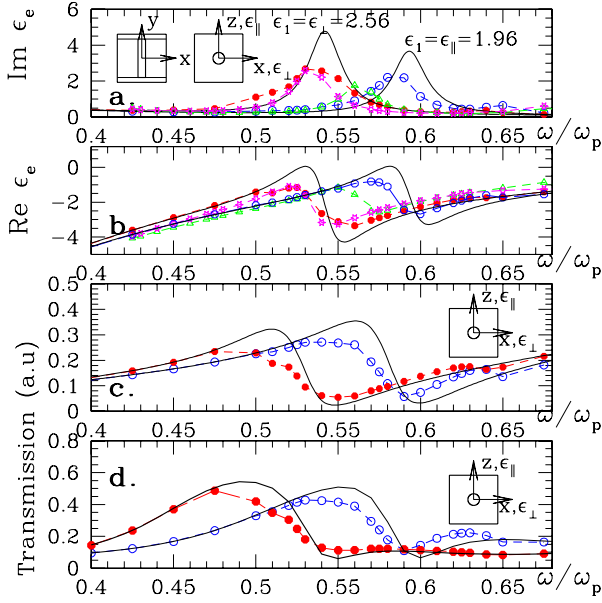


Fig. 2. (Color online) (a) $\text{Im } \epsilon_{\perp}^{(e)}$ and $\text{Im } \epsilon_{\parallel}^{(e)}$ vs. ω/ω_p . (b) $\text{Re } \epsilon_{\perp}^{(e)}$ and $\text{Re } \epsilon_{\parallel}^{(e)}$ vs. ω/ω_p . (c) Transmission coefficient T (see Eq. (16)) vs. frequency ω , for different polarizations $\mathbf{E} \parallel x$ and $\mathbf{E} \parallel y$. Full curves: analytical results using a Clausius-Mossotti approximation (cf. Eqs. (11)). Points connected by the dashed lines: numerical results using the method of reference [6] for a square array of right circular cylindrical holes. Open triangles (Δ) and stars ($*$): 3D calculations using the unit cell whose side and top views are shown in insets to (a). Solid (\bullet) and open (\circ) circles: results obtained from 2D calculations. In all cases, we take $R/a = 0.1$ (ratio of hole radius to lattice constant), $\omega_p \tau = 40$, and $\omega_p h/c = 5/3$. (d) Similar to (c), but the transmission coefficient $T = |d(\omega)|^2$ is calculated for the case of the perforated film dipped into a large pool of the NLC (see Fig. 1b).

3 Numerical results

In Figure 2a, we show the calculated $\text{Im } \epsilon_e(\omega)$ for several cases. In all cases, we assume that the cylindrical holes are filled by BEHA, and that $\hat{n} \parallel \hat{x}$. For the metal film, we assume $\omega_p \tau = 40$. The filled curves without points are the two principal components of $\text{Im } \epsilon_e$, denoted $\text{Im } \epsilon_{e,\parallel}$ and $\text{Im } \epsilon_{e,\perp}$, corresponding to the in-plane components parallel and perpendicular to \hat{n} , as obtained in the MG approximation. We use the dielectric properties of BEHA and assume volume fraction $p = 0.031$ (i.e., the ratio of hole radius to lattice constant $R/a = 0.1$). As in the previous Section, we take the $\hat{n} \parallel \hat{x}$, while cylindrical inclusions are assumed $\parallel \hat{y}$.

The filled and open circles in Figure 2a denote the same quantities, but now for a square lattice of holes in the shape of right-circular cylinders, again of volume fraction $p = 0.031$. This value corresponds to holes of radius $0.1a$ on a square lattice of lattice constant a . In this case, $\text{Im } \epsilon_{\parallel}$ and $\text{Im } \epsilon_{\perp}$ are calculated by a Fourier expansion technique mentioned above, and described in detail in reference [5].

Two geometries were used: three-dimensional (3D) sandwich-like system mimicking the 3D films of finite

thickness (side and top views of the unit cell of this composite are shown in the insets to Fig. 2a) and a system with infinitely long cylindrical holes, which reduces the 3D problem to a two-dimensional (2D) one: when the length of the cylinder l is equal to the linear dimension, a , of the unit cell (see inset to Fig. 2a), then each Fourier component $\theta_{\mathbf{g}} = \int_{\text{unit cell}} \theta(\mathbf{r}) e^{-i\mathbf{g}\cdot\mathbf{r}} d\mathbf{r}$ (of the characteristic $\theta(\mathbf{r})$ -function describing the cylinder) vanishes for each reciprocal lattice vector

$$\mathbf{g} = (g_x, g_y, g_z) = \frac{2\pi}{a}(m_x, m_y, m_z) \quad (14)$$

except for components with values $g_y = 0$ only (here m_x, m_y, m_z are the arbitrary integers). This can be seen directly from the analytical form [6, 7]: $\theta_{\mathbf{g}} = (4\pi/a^3 g_{\perp}) R J_1(R g_{\perp}) \sin(g_y l/2)/g_y$, where $g_{\perp} = \sqrt{g_x^2 + g_z^2}$ and $J_1(x)$ is a Bessel function (note that cylinder's symmetry axis is parallel to y -axis).

The effective permittivity $\epsilon_{\text{film}}^{(e)}$ of the 3D film of the finite thickness can be extracted from the *total* effective permittivity of the sandwich-like systems (shown in the insets to Fig. 2a), $\epsilon_{\text{tot}}^{(e)}$, using the exact relation for a system of parallel slabs aligned along the electric field of the incident wave \mathbf{E} (see e.g., Ref. [30])

$$\epsilon_{\text{tot}}^{(e)} = p_{\text{slab}} \epsilon_m + p_{\text{film}} \epsilon_{\text{film}}^{(e)}, \quad (15)$$

where p_{slab} and p_{film} are the volume fractions of the subsystem with a cylindrical hole of finite length (denoted by sub-index ‘‘film’’) and the subsystem of two (upper and lower) homogeneous slabs (denoted by sub-index ‘‘slab’’), respectively. ϵ_m in equation (15) is the permittivity of these slabs as given by equation (4), p_{slab} and p_{film} were taken of the values $p_{\text{slab}} = 0.2$ and $p_{\text{film}} = 1 - p_{\text{slab}} = 0.8$, respectively.

In the case of a 3D system, we include 5831 Fourier components of the electrostatic potential with arbitrary integers m_x, m_y, m_z (see Eq. (14)) ranging from -9 up to $+9$ in each direction (so that the total number of \mathbf{g} vectors reaches the value $18^3 - 1 = 5831$). The dashed lines simply connect the calculated points.

In the case of a 2D system we include 6399 Fourier components of the electrostatic potential with 2D reciprocal lattice vectors $\mathbf{g} = (2\pi/a)(m_x, m_z)$, the arbitrary integers of which ranging from -40 up to $+40$ in each directions (so that the total number of \mathbf{g} vectors reaches the value $80^2 - 1 = 6399$).

Despite the total numbers of Fourier components in both 2D and 3D cases had the same order of magnitude, in the 2D case all components were used for describing the circular hole perpendicular to the xz -plane (note that the resonance is very sensitive to the hole's shape), while in 3D only some of Fourier components ($18^2 - 1 = 323$) were used in this way. We prefer, therefore, to get the effective values of the permittivity tensor $\hat{\epsilon}_e$ from the 2D calculations, while we will take the film thickness into account by using the proper analytical expressions for optical light transmission (see Eqs. (16)–(21) below).

In the regions far away from the resonance, the results of both 3D and 2D calculations are in good quantitative agreement with each other as well as with our MG analytical predictions. However, in the very near of the resonance there is a small discrepancy between them. In order to get a better agreement, one needs to use in the calculations a larger number of Fourier components, which is beyond our computer capabilities.

In Figure 2b, we show the $\text{Re}\epsilon_e(\omega)$ for the same cases as in Figure 2a, as calculated by the MG approximation and by the Fourier expansion technique. Finally, in Figure 2c, we show the calculated transmission coefficient T for the dielectric functions presented in Figures 2a and 2b. The dependence of the transmission coefficient T on frequency ω , (as well as on the wave length λ) for different film thicknesses can be obtained from the effective value ϵ_e using the known expression [29,34] for $T = |d|^2$:

$$d = \frac{1 - r_{12}^2}{\exp(-i\psi) - r_{12}^2 \exp(i\psi)}, \quad (16)$$

where $r_{12} = (1 - s)/(1 + s)$, $s = \sqrt{\epsilon_e(\omega)}$, $\psi = (\omega/c)hs = (\omega/\omega_p)(\omega_p h/c)s$, and h is the film thickness. We assume that the light is incident from, and transmitted into, a material with dielectric constant $\epsilon = 1$.

Equation (16) can be easily extended to the case of \mathcal{N} layers or $N = \mathcal{N} + 2$ media system (\mathcal{N} layers plus two semi-infinite media on both sites), as follows:

$$d = \prod_{i=N-1}^1 \left(\frac{e^{i\psi_i} + R_i e^{-i\psi_i}}{1 + R_{i+1}} \right), \quad (17)$$

$$R_i = \frac{(1 + R_{i+1}) - \kappa_{i+1}(1 - R_{i+1})}{(1 + R_{i+1}) + \kappa_{i+1}(1 - R_{i+1})} e^{2i\psi_i}, \quad (18)$$

$$\psi_i = \frac{\omega}{c} h_i s_i = \frac{\omega}{\omega_p} \frac{\omega_p h_i}{c} s_i, \quad (19)$$

$$\kappa_i = k_{iz}/k_{i-1z}, \quad (20)$$

$$k_{iz} = \frac{\omega}{c} \sqrt{\epsilon_i}. \quad (21)$$

Here $\prod_{i=N-1}^1$ denotes the product from $i = N - 1$ to $i = 1$, $s_i = \sqrt{\epsilon_i^{(e)}(\omega)}$, and h_i is the thickness of i -th media, excepting the first one, for which $h_1 = 0$, and $\psi_1 = 0$ (note also that $R_N = 0$). For $N = 3$ the result of equations (17)-(21) coincides with that of equation (16).

A number of features are evident from Figure 2. First, both the MG calculation and the Fourier calculation carried out by the method of reference [5] (SB) show that $\text{Im}\epsilon_e(\omega)$ has sharp peaks which are split by the anisotropy of the material in the cylindrical holes. These peaks correspond to the SP resonances mentioned above. The splitting is quite pronounced (around $0.06\omega_p$ for the MG calculation, and slightly smaller for the Fourier one), and should be readily observable in experiment. Secondly, the SP resonances are slightly shifted in the SB calculation relative to those obtained in the MG approximation. Since the MG approximation is more appropriate for a random distribution of holes, these results show that, even for this small volume fraction, the effects of lattice periodicity are quite noticeable, though they must vanish in

the limit of very small volume fraction. In addition, the lower-frequency SP peak in the SB calculation appears to be partially split; however, it is possible that this splitting might be absent if still more Fourier components were used in the computation. In both approximations, $\text{Re}\epsilon_e(\omega)$ is negative for all frequencies considered, and is an increasing function of frequency at low ω , as expected for a metallic film.

The transmission coefficient $T(\omega)$ (see Fig. 2c and Eq. (16)), shows the characteristic “extraordinary transmission” peaks expected on the basis of Figures 2a, 2b. Both approximations show rather sharp SP peaks in the transmission, which occur at different frequencies depending on the polarization of the incident radiation. They occur at slightly different frequencies from the SP peaks themselves. This is the expected behavior, since the SP peaks correspond to *absorption* maxima. In fact, the transmission peaks occur at frequencies which correspond closely to the maxima in the *real part* of $\epsilon_e(\omega)$ for the chosen polarization. The maxima in $T(\omega)$ are indeed extraordinary, reaching the range of 20%, even though the holes themselves occupy only about 3% of the film volume fraction. The curves are obtained for the dimensionless value $\xi = \omega_p h/c = 5/3$. When for $\omega_p = 10^{15}$ rad/s (a typical for the Al value [30]) it corresponds to the film thickness $h = 0.5 \mu\text{m}$ (cf. with 200–300 nm in the experiments [1,2,4,33,35]). The wave length of the light corresponding to the resonance frequency ω_{sp} (see Eqs. (12, 13)) is of the order $\lambda = 2\pi c/\omega_{sp} \sim 3770$ nm. Since we have used the quasistatic approximation, the wavelength should be much larger than the hole (cf. this value of the wave-length $\lambda \sim 3770$ nm with the hole sizes used in the experiments ~ 150 – 700 nm, see Refs. [33,35]). We emphasize that in our calculations we have not used any absolute values (except for the film thickness), but only relative ones — namely, the ratio of the hole diameter to the distance between holes. If in Figure 2 we were to consider a smaller film thickness, then the transmissivity coefficient, T definitely would be increased. In Figure 3 we show the data, presented in Figure 2c, in terms of wave-length λ .

In Figure 2d we show results analogous to those of Figure 2c, but for the case of three layers (see Fig. 1b), calculated using equations (17)-(21). The transmissivity in this case depends also on thicknesses of both the homogeneous NLC layers (those on either side of the metallic film). In the case shown in Figure 2d we used thicknesses $h_2 = h_4 = 3h_3$.

To illustrate the effects of a larger anisotropy, we show in Figure 4 the same quantities, but calculated for a hypothetical film in which the holes are filled with an anisotropic dielectric with dielectric constants $\epsilon_{\parallel} = 4$, $\epsilon_{\perp} = 1$. The effects seen in Figure 2 are still present, but are significantly amplified by the larger anisotropy. There are still strong “extraordinary” peaks in the transmission coefficients corresponding to maxima in the real parts of $\epsilon_e(\omega)$ as in Figure 2c.

To investigate the effects of a larger volume fraction of holes, we have carried out similar calculations for

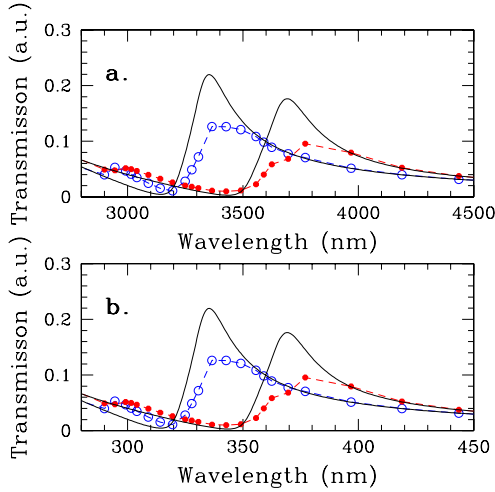


Fig. 3. (Color online) The same as Figure 2c, but vs. wavelength λ . (a) $\omega_p = 10^{15}$ rad/s; (b) $\omega_p = 10^{16}$ rad/s.

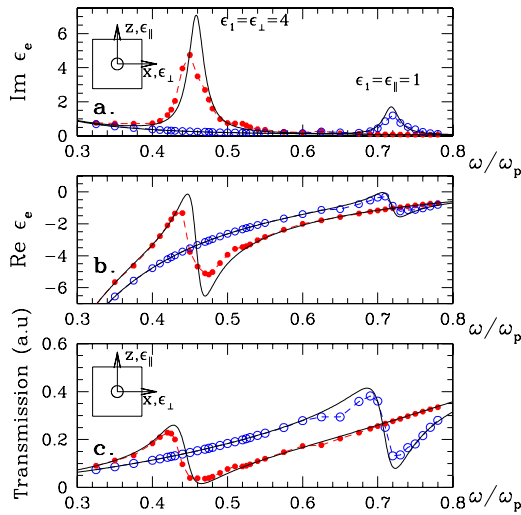


Fig. 4. (Color online) Same as Figure 2, but for a hypothetical material with $\epsilon_{\parallel} = 1$, $\epsilon_{\perp} = 4$, $\omega_p h/c = 50/3$ (see explanation to Eq. (16) and Fig. 2), i.e. $h = 0.5 \mu\text{m}$ for Al.

$p = 0.126$. The results are shown in Figure 5. The features are similar to those seen in Figure 2, except that, in the SB calculation the SP peaks are significantly more broadened than at $p = 0.031$. By contrast, there is no increase in the widths of the SP peaks calculated in the MG approximation. Also, the transmission peaks for the smaller p could be viewed as more “extraordinary” than those at $p = 0.126$ because the ratio of the maximum T to the areal fraction of holes is much greater at the smaller value of p . However, in both cases, the fraction of power transmitted is far larger than the hole areal fraction.

4 Discussion

The present work suggests that extraordinary transmission through perforated metal films can easily be controlled by filling the holes with an NLC such as BEHA.

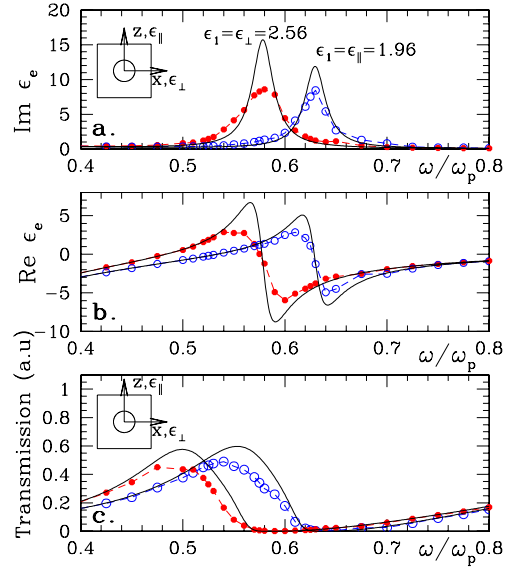


Fig. 5. (Color online) Same as Figure 1, but for $p = 0.126$. $\omega_p h/c = 60/3$ (see explanation to Eq. (16) and Fig. 2), i.e. $h = 0.6 \mu\text{m}$ for Al.

One control scheme might work as follows. The metal screen would be dipped into a pool of NLC (at a temperature T below the nematic-to-isotropic transition at T_c). This would cause the NLC to penetrate into the holes of the perforated film and also to form layers of homogeneous NLC on the two sides of the film. A static electric field \mathbf{E}_0 would then be applied parallel to the film, causing the NLC director to line up parallel to the applied electric field outside the holes, and also, since the free energy of the NLC would be minimized if the director is everywhere pointing in the same direction, both within the holes and in the two layers. A second scheme would be the following (if one could introduce NLC into the holes within the metal screen but not outside the screen). In this case, a static *magnetic* field be applied parallel to the film surface. For both schemes, since the transmission would differ substantially for \hat{n} parallel and perpendicular to the polarization of the incident wave, $T(\omega)$ through the film could be controlled simply by rotating \mathbf{E}_0 or \mathbf{H}_0 . Thus, we would have the possibility of a film which could be converted from nearly transparent to nearly opaque, simply by rotating an applied field. Such a material could have many possible applications.

We conclude with a final remark. Our method of calculation assumes that the lattice constant of the hole lattice is small compared to the wavelength of light. Nonetheless, we believe that the effects predicted here for such lattice constants should persist even for lattice constants comparable to a wavelength, as in most experiments to date. One reason for our belief is that, even though the spacing and wavelength are comparable, the electric field of a normally incident plane wave is uniform in the direction transverse to the wave propagation. The extension of the present calculations to this regime would be challenging, since the computation of transmission through

a perforated metallic film is quite intricate when the wavelength and lattice constant are comparable[3]. It would be of great interest if the present calculations could be extended into this regime.

This work has been supported by NSF Grant DMR04-13395, by the US/Israel Binational Science Foundation, and the KAMEA Fellowship program of the Ministry of Absorption of the State of Israel. We also benefited from the computational facilities of the Ohio Supercomputer Center and the Israel Inter-University Centers. We thank Dr. Sung Yong Park, Prof. M.I. Shliomis and Prof. A.N. Zakhlevnykh for valuable conversations.

References

1. T.W. Ebbesen, H.H.J. Lezec, H.F. Ghaemi, T. Thio, P.A. Wolff, *Nature* **391**, 667 (1998)
2. H.F. Ghaemi, T. Thio, D.E. Grupp, T.W. Ebbesen, H.J. Lezec, *Phys. Rev. B* **58**, 6779 (1998)
3. J.A. Porto, F.J. Garcia-Vidal, J.B. Pendry, *Phys. Rev. Lett.* **83**, 2845 (1999)
4. L. Martin-Moreno, F.J. Garcia-Vidal, H.J. Lezec, K.M. Pellerin, T. Thio, J.B. Pendry, T.W. Ebbesen, *Phys. Rev. Lett.* **86**, 1114 (2001)
5. Y.M. Strelniker, D.J. Bergman, *Phys. Rev. B* **59**, R12763 (1999)
6. Y.M. Strelniker, D.J. Bergman, *Phys. Rev. B* **50**, 14001 (1994)
7. D.J. Bergman, Y.M. Strelniker, *Phys. Rev. B* **49**, 16256 (1994)
8. D.J. Bergman, Y.M. Strelniker, *Phys. Rev. Lett.* **80**, 857 (1998)
9. D.M. Newman, M.L. Wears, R.J. Matelon, *Europhys. Lett.* **68**, 692 (2004)
10. G. Duchs, G.L.J.A. Rikken, T. Grenet, P. Wyder, *Phys. Rev. Lett.* **87**, 127202 (2001)
11. L.E. Helseth, *Phys. Rev. B* **72**, 033409 (2005)
12. A. Garcia-Martin, G. Armelles, S. Pereira, *Phys. Rev. B* **71**, 205116 (2005)
13. M. Diwekar, V. Kamaev, J. Shi, Z.V. Vardeny, *Appl. Phys. Lett.* **84**, 3112 (2004)
14. M. Golosovsky, Y. Neve-Oz, D. Davidov, *Phys. Rev. B* **71**, 195105 (2005)
15. B. Sepulveda, L.M. Lechuga, G. Armelles, *J. Lightwave Technology* **24**, 945 (2006)
16. A. Boardman, N. King, Y. Rapport, L. Velasco, *New Journal of Physics* **7**, 191 (2005)
17. K. Busch, S. John, *Phys. Rev. Lett.* **83**, 967 (1999)
18. J. Müller, C. Sönnichsen, H. von Poschinger, G. von Plessen, T.A. Klar, J. Feldmann, *Appl. Phys. Lett.* **81**, 171 (2002)
19. S.Y. Park, D. Stroud, *Appl. Phys. Lett.* **85**, 2920 (2004)
20. S.Y. Park, D. Stroud, *Phys. Rev. Lett.* **94**, 217401 (2005)
21. D. Kang, J.E. Maclellan, N.A. Clark, A.A. Zakhidov, R.H. Baughman, *Phys. Rev. Lett.* **86**, 4052 (2001)
22. H. Takeda, K. Yoshino, *Phys. Rev. B* **66**, 115207 (2002)
23. In reality, the orientation of the director within the cylindrical hole is controlled by a balance between surface forces, the various elastic constants of the NLC, and any applied static electric or magnetic fields. However, in carrying out of our calculations, we neglect the influence of the cylindrical hole walls on the liquid crystal. In a realistic hole, the walls might locally reorient \hat{n} , causing it to be locally perpendicular to the wall. This effect has not been included in our calculations. As discussed by Lubensky et al. [T.C. Lubensky, D. Pettey, N. Currier, H. Stark, *Phys. Rev. E* **57**, 610 (1998)], this effect is typically small, for composites with length scales less than around $0.3 \mu\text{m}$. For composites with larger length scales, such reorientation might need to be considered
24. P.G. de Gennes, J. Prost, *The Physics of Liquid Crystals* (Clarendon Press, Oxford, 1991)
25. V. Freedericksz, V. Zolina, *Z. Krist. B* **72**, 255 (1931); *Trans. Faraday Soc.* **29**, 919 (1933)
26. Y.M. Strelniker, D.J. Bergman, *Eur. Phys. J. AP* **7**, 19 (1999)
27. D. Stroud, *Phys. Rev. B* **12**, 3368 (1975)
28. D.J. Bergman, Y.M. Strelniker, *Phys. Rev. B* **60**, 13016 (1999)
29. L.D. Landau, E.M. Lifshitz, L.P. Pitaevskii, *Electrodynamics of Continuous Media*, 2nd edn. (Pergamon, Oxford, 1993)
30. D.J. Bergman, D. Stroud, *Solid State Physics* **46**, 147 (1992)
31. L.M. Blinov, V.A. Kizel, V.G. Rumyantsev, V.V. Titov, *J. Phys.* **36**, Colloq. C1, C1-69 (1975)
32. L.M. Blinov, V.G. Chigrinov, *Electro-Optic Effects in Liquid Crystal Materials* (Springer-Verlag, New York, 1994)
33. C. Sönnichsen, A.C. Duch, G. Steininger, M. Koch, G. von Plessen, *Appl. Phys. Lett.* **76**, 140 (2000)
34. A.M. Dykhne, A.K. Sarychev, V.M. Shalaev, *Phys. Rev. B* **67**, 195402 (2003)
35. D.S. Kim, S.C. Hohng, V. Malyarchuk, Y.C. Yoon, Y.H. Ahn, K.J. Yee, J.W. Park, J. Kimm, Q.H. Park, C. Lienau, *Phys. Rev. Lett.* **91**, 143901 (2003)
36. F.I. Baida, D. Van Labeke, *Phys. Rev. B* **67**, 155314 (2003)